



Progressive collapse analysis of steel truss bridges and evaluation of ductility

Kazuhiro Miyachi ^a, Shunichi Nakamura ^{b,*}, Akihiro Manda ^a

^a Civil Engineering Course, Graduate School, Tokai University, 4-1 Kitakaname, Hiratsuka, Japan

^b Dept. of Civil Engineering, Tokai University, 4-1 Kitakaname, Hiratsuka, Japan

ARTICLE INFO

Article history:

Received 31 January 2012

Accepted 29 June 2012

Available online 3 August 2012

Keywords:

Steel truss bridges
Progressive collapse
Ultimate strength
Large deformation
Elastic–plastic
Ductility

ABSTRACT

Deteriorated steel truss bridges have caused catastrophes in the USA and Japan. Progressive collapse analysis is carried out for three continuous steel truss bridge models with a total length of 230.0 m using large deformation and elastic plastic analysis. The analysis is to clarify how the live load intensity and distribution affect ultimate strength and ductility of two steel truss bridge models, Bridge Model A with a span ratio of 1:2:1 and Bridge Model B with a span ratio of 1:1.3:1. Sizes and steel grades of the truss members are determined so that they are within the allowable stress for the design dead and live loads. After the design load is applied, the live load is increased until the bridge model collapses. Although the collapse process differs depending on live load distribution and span length ratio, both steel truss bridge models collapse due to buckling of compression members. When the live load is fully applied in the center span, the span ratio does not affect the ultimate strength which is sufficiently high and the model bridge is safe. When the live load is applied in the side span, the model bridge with a longer side span has higher ultimate strength. When the live load is applied near the intermediate support, the model bridge with a longer center span has higher ultimate strength. As for the ductility factor which is defined by the ultimate load over the yield load, Bridge Model B is in general more ductile than Bridge Model A. This leads to the fact that the center and side span length ratio of Bridge Model B with more commonly used dimensions is rational. This study clarifies the collapse process, buckling strength, and influences of live load distribution and the span ratio on a steel truss bridge.

© 2012 Elsevier Ltd. All rights reserved.

1. Introduction

The steel truss bridge I-35W over the Mississippi River in Minneapolis, Minnesota, United States, suddenly collapsed on the 1st of August 2007 and there were many victims in this disaster [1,2]. The report about the collapse of the I-35W clarifies that dead load increased several times due to repair and reinforcement of the slab, and the thickness of gusset plate was half of the design value. In addition, on the day of the I-35W collapse, there were construction materials and heavy machinery on the truss bridge for the maintenance. These factors are the possible causes of the collapse of the I-35W.

In Japan, there are many aging truss bridges as well and they need prompt inspection, reinforcement and maintenance. On the Kiso River Bridge and the Honjo Bridge the diagonal member penetrates the RC slab and it fractured because of corrosion [3]. Nagatani et al. studied the redundancy of truss bridges [4]. Kasano et al. focused on the gusset plate and clarify that the thinner gusset plate with initial deformation increases strain and may trigger cracking [5].

However, there is no research on how the live load intensity and distributions affect the collapse process, the final deformation and the ultimate strength. There is also no research about the influence of the main and side span length ratio. In this research it is intended

to clarify how these factors affect three continuous span steel truss bridges of the fixed span length. As a reminder, this study does not aim to clarify the collapse mechanism of I-35W but to evaluate the ultimate strength of general steel truss bridges. It is highly difficult to find the collapse loads and mechanism because non-linearity of materials and geometry must be considered in complicated indeterminate structures. Therefore, structural models are simplified as two dimensional and truss members are directly connected without gusset plates. Progressive collapse analysis is conducted for four live load cases on the two bridge models with different span ratios using large deformation elastic–plastic analysis. Then, the collapse process, the collapse load and the final deformation are obtained. How the span ratio and the live load distribution affect the ductility of steel truss bridges is also studied.

2. Structural model

Figs. 1 and 2 show the bridge model, a three continuous span Warren truss bridge with a total length of 230 m. Bridge Model A has a span ratio of 1:2:1 with a center span of 115 m, a side span of 57.5 m and a height of 10 m. Although Bridge Model A has nearly the same dimensions as the I-35W, the objective of this study is not to investigate the causes of the collapse of the I-35W and the truss height and width of the model bridges are different. The objective

* Corresponding author. Tel.: +81 463 58 1211; fax: +81 463 50 2170.
E-mail address: snakamu25@gmail.com (S. Nakamura).

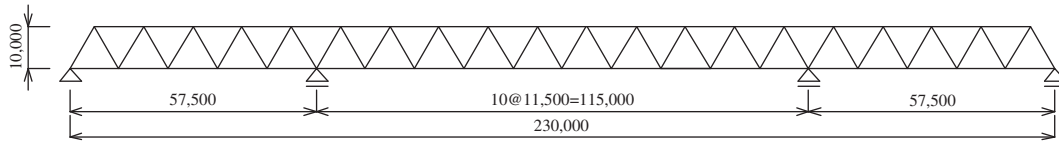


Fig. 1. Side view of Bridge Model A (unit: mm).

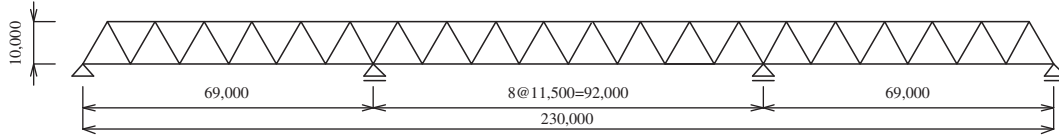


Fig. 2. Side view of Bridge Model B (unit: mm).

of this study is to conduct progressive collapse analysis to clarify the effects of live load distribution and span ratio.

Bridge Model B has a span ratio of 1:1.3:1 with a center span of 92 m, a side of 69 m and a height of 10 m. The length of each upper chord and lower chord is 11.5 m. In general, for continuous three-span truss bridges, the span ratio of Bridge Model B is more commonly used than that of Bridge Model A.

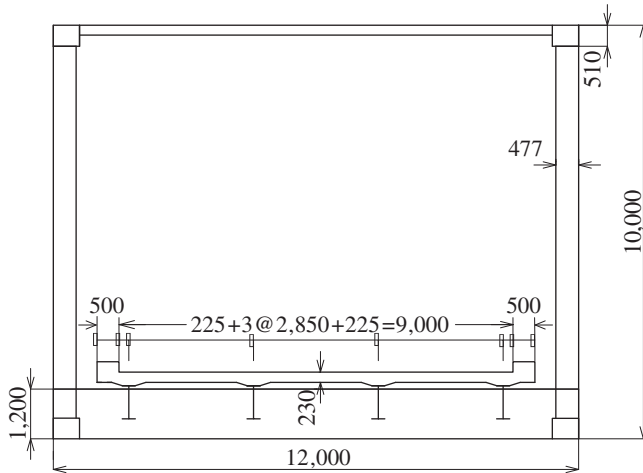


Fig. 3. Cross section of bridge model.

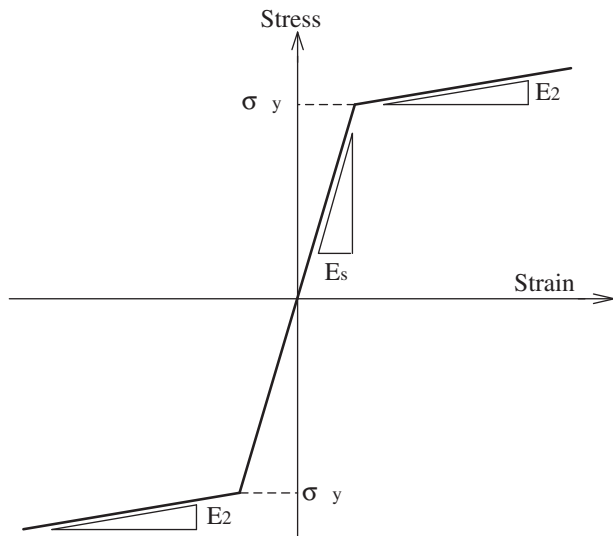


Fig. 4. Stress and strain relation of steel.

Fig. 3 shows the cross section of structural members and deck system. RC slab is assumed for the bridge deck. Two steel grades in Japanese Industrial Standard are used [6]: SS490Y with tensile strength of 490 MPa and SS400 with tensile strength of 400 MPa. The assumed stress strain curve is shown in Fig. 4. Table 1 shows yield stress, yield strain and elastic and plastic modulus of the assumed two grades of steel. The ultimate strain is set at 10%, which is a conservative value.

Fig. 5 shows typical cross sections of the structural members: upper chord, lower chord and diagonal member. To simplify this truss bridge model, all diagonal members are assumed to have rectangular cross sections. Sizes and grades of steel members are determined so that the design stress is within the allowable stress specified in the Japanese current design specification [6].

3. Preliminary design of truss members

Static structural analysis was conducted for the dead load (P_D) and the design live loads (P_L : combination of uniformly distributed of 3.5 kN/m^2 and concentrated loads of 10.0 kN/m^2 with a longitudinal width of 10 m), and sectional forces and deformations were obtained. The design live load of B-type of the Japanese specifications for road bridges is adopted in this study. Four load cases, $P_D + P_{L1}$, $P_D + P_{L2}$, $P_D + P_{L3}$ and $P_D + P_{L4}$ are considered in this progressive collapse analysis. As shown in Fig. 6, P_{L1} is the live load distributed in full spans (Case-1), P_{L2} is that distributed only in the center span (Case-2), P_{L3} is that distributed only in the side span (Case-3), and P_{L4} is that applied near the intermediate support B (Case-4). Case 4 is chosen because heavy machinery and construction materials were near the intermediate support when the I35-W collapsed.

The analytical model is a two dimensional model and only the main truss structure (Figs. 1 and 2) is considered. The dead and live loads are assumed to be loaded on the full deck width and applied equally to both truss planes. Therefore, the eccentric loads are not applied and torsion is not considered. If the eccentric loads are applied, it would affect the cross beams or lateral truss members. However, the authors predict that it would not lead to the catastrophic failure of the whole truss bridge, which needs further study to be proved. The design dead load per unit length of the truss is 60.56 kN/m . The design live load intensity is a combination of 14.67 kN/m (uniformly distributed loads), and 46.59 kN/m (concentrated loads with length of 10 m).

Table 1
Mechanical properties of steel.

Steel Grade	SM490Y	SS400
Tensile strength (N/mm^2)	$\sigma_u = 490$	$\sigma_u = 400$
Yield stress (N/mm^2)	$\sigma_y = 355$	$\sigma_y = 235$
Yield strain (μ)	$\epsilon_y = 1775$	$\epsilon_y = 1175$
Elastic and plastic modulus (N/mm^2)	$E_s = 2.0 \times 10^5$	$E_s = 2.0 \times 10^5$
	$E_2 = 2.0 \times 10^5$	$E_2 = 2.0 \times 10^5$

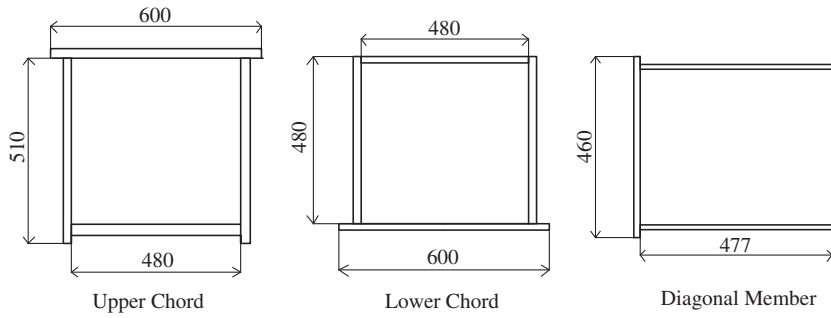


Fig. 5. Cross sections of truss members.

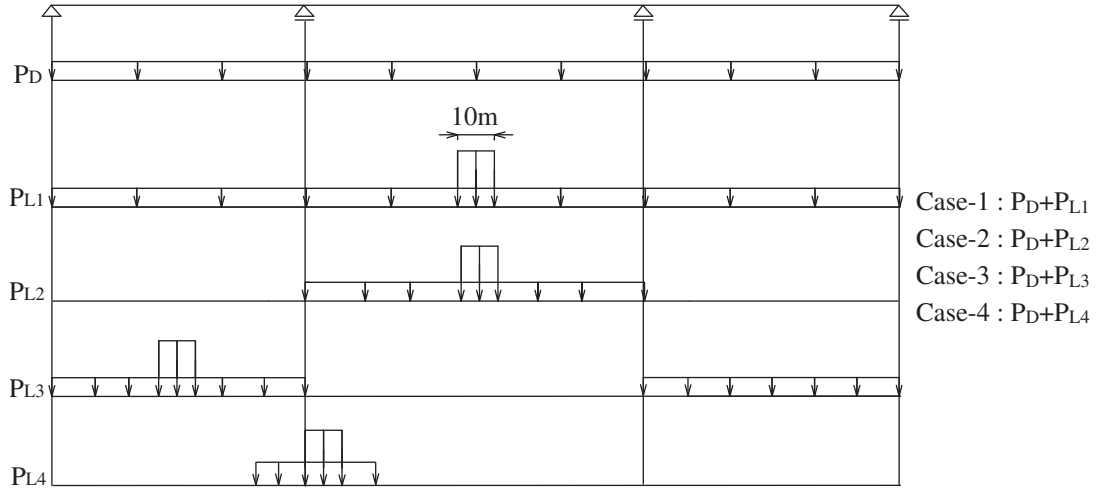


Fig. 6. Dead and live load cases.

Thickness and steel grade of the truss members are then determined by the allowable stress method for the two bridge models. Figs. 7 and 8 show the location of the designed members. All the

truss members are categorized into 10 groups. Each group has the same cross section with the same steel grade. Two steel grades based on the Japanese Industrial Standard [6] are assumed: SS400

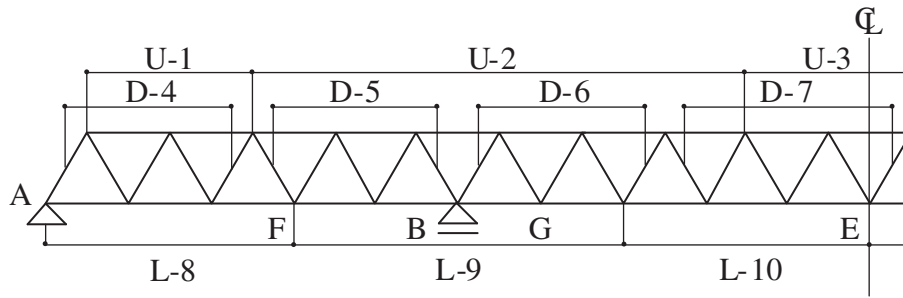


Fig. 7. Truss members of Bridge Model A.

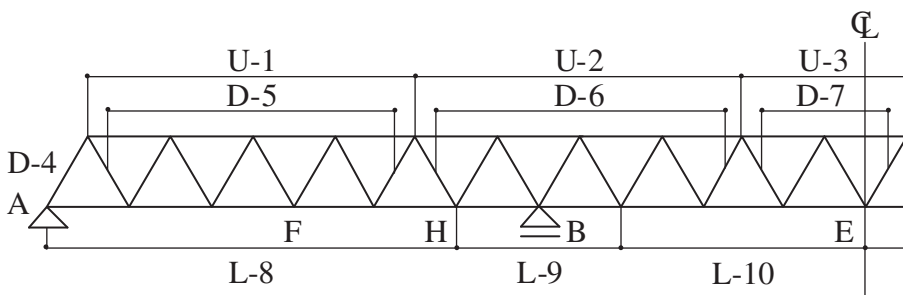


Fig. 8. Truss members of Bridge Model B.

Table 2
Truss members designed by allowable stress methods (Bridge Model A).

Size (mm)			Steel grade	Member no.	σ/σ_a			
UFlg	Web	LFlg			$P_D + P_{L1}$	$P_D + P_{L2}$	$P_D + P_{L3}$	$P_D + P_{L4}$
600*9	510*9	480*13	SS400	U-1	0.13	0.10	0.82	0.03
600*15	510*15	480*17	SM490Y	U-2	0.95	0.93	0.77	0.81
600*25	510*25	480*30	SM490Y	U-3	0.87	0.89	0.57	0.66
460*22	433*11	460*22	SS400	D-4	0.47	0.2	0.89	0.33
460*22	433*11	460*22	SM490Y	D-5	0.84	0.73	0.84	0.69
460*22	433*20	460*22	SM490Y	D-6	0.999	0.999	0.76	0.95
460*22	433*20	460*22	SS400	D-7	0.84	0.84	0.58	0.51
480*9	480*9	500*9	SS400	L-8	0.41	0.82	0.28	0.45
480*20	480*20	600*16	SM490Y	L-9	0.99	0.99	0.74	0.84
480*18	480*18	600*14	SM490Y	L10	0.89	0.92	0.59	0.69

Table 3
Truss members designed by allowable stress methods (Bridge Model B).

Size (mm)			Steel grade	Member no.	σ/σ_a			
UFlg	Web	LFlg			$P_D + P_{L1}$	$P_D + P_{L2}$	$P_D + P_{L3}$	$P_D + P_{L4}$
600*22	510*22	480*27	SS400	U-1	0.56	0.32	0.91	0.41
600*18	510*18	480*20	SS400	U-2	0.97	0.91	0.82	0.81
600*15	510*15	480*20	SM490Y	U-3	0.81	0.87	0.44	0.60
460*11	455*10	460*11	SM490Y	D-4	0.69	0.48	0.85	0.52
460*22	433*9	460*22	SS400	D-5	0.74	0.65	0.82	0.59
460*22	433*11	460*22	SM490Y	D-6	0.95	0.95	0.71	0.93
460*9	459*9	460*9	SS400	D-7	0.81	0.81	0.46	0.26
480*14	480*14	600*11	SS400	L-8	0.58	0.36	0.85	0.43
480*22	480*22	600*18	SM490Y	L-9	0.86	0.85	0.64	0.72
480*16	480*16	600*14	SS400	L10	0.80	0.87	0.43	0.63

(tensile strength of 400 MPa, yield stress of 245 MPa, allowable tensile stress of 140 MPa) and SM490Y (tensile strength of 490 MPa, yield stress of 365 MPa, allowable tensile stress of 210 MPa). Tables 2 and 3 show ratios of the design stress over the allowable stress of upper and lower flanges and web plates in the four live load cases. These tables show that all the member stresses are over 80% of the allowable stress and the cross sections of truss members seem to be practically acceptable.

4. Analytical results of progressive collapse analysis of Bridge Model A

Progressive collapse analysis is conducted for Bridge Model A and the results are shown in this section. The analytical model is two dimensional and the whole skeleton is shown in Figs. 1 and 2. Each truss member is divided into 14 sections along the member axis (Fig. 9). A cross section of truss members is divided into fiber elements; the flange is divided into five layers in depth and five slices in width, and the web is divided into fifteen layers in depth and fifteen slices in width (Fig. 10). Each fiber follows the stress–strain relation of Fig. 4.

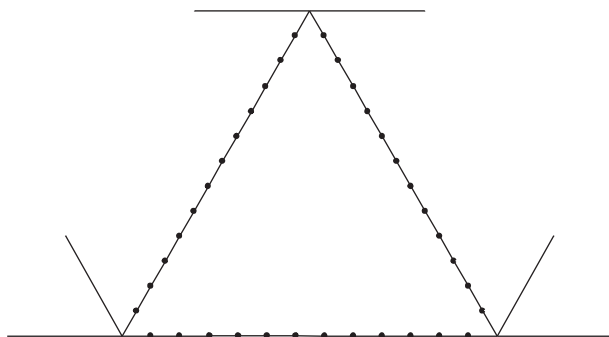


Fig. 9. Nodes in truss members.

The analytical procedure is as follows. First the dead load is applied, and then the live load is applied incrementally until the bridge collapses. This can be expressed as $P_D + k P_L$, where k is the load amplification coefficient. The analysis includes elastic–plastic properties of steel and large deformation effect. Calculation was carried out by a FEM program, FORUM8 FRAME (3D).

Collapse processes and final deformations in the four live load cases are shown in Fig. 11. In Case-1, the upper chord at support B became yield in tension at first. Then, the lower chord became yield in tension at the span center. Next, compression yield appeared near the intermediate support and in the span center. Finally, when the load amplification coefficient k reached 4.69, the upper chord buckled at the span center. The maximum tensile strain was 2.3% at the upper chord at support B. At collapse the deflection at the center span is very large but the deflection at the side span is small.

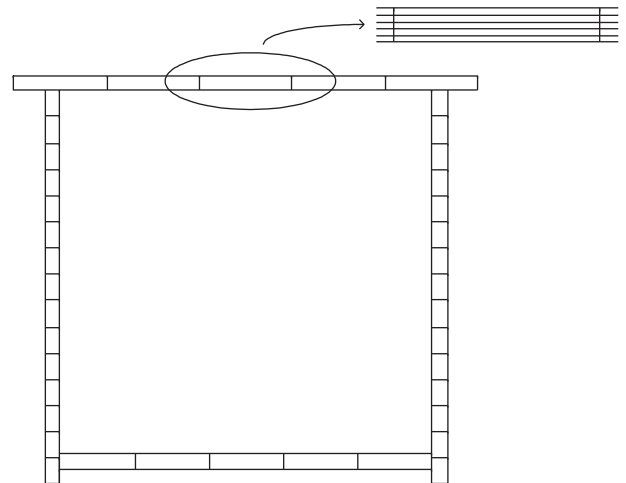


Fig. 10. Fiber elements in a box section.

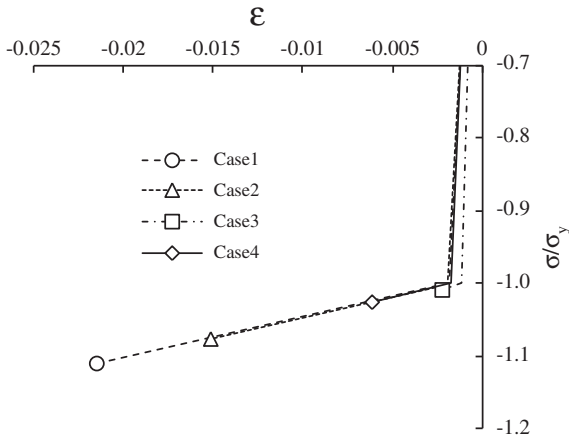


Fig. 12. Compressive stress and strain of Bridge Model A.

Fig. 12 shows the compressive stress and strain relation of the buckled members. To compare steel members with different yield strength σ_y , the vertical axis is a non-dimensional parameter σ/σ_y . The bridge collapsed at σ/σ_y of -1.11 in Case-1, -1.08 in Case-2, -1.02 in Case-3 and -1.01 in Case-4. These results show that the model truss bridge collapses because of buckling which occurs just after it reaches yield stress.

Fig. 13 shows the relationship of applied loads and vertical displacements at the critical points. The load amplification coefficient k instead of the load itself is used so as to compare the four live load cases. Lateral axis is a non-dimensional parameter δ/δ_y , vertical displacement divided by the yield displacement when a first member yields. The value of δ/δ_y at the buckling, whose points are marked in the figure, is 5.10, 4.64, 3.86 and 1.27 in Cases-1, 2, 3, 4, respectively. In all the cases vertical displacements sharply increase when they reach yield loads. In Cases-1 and 2, vertical displacements increase further after buckling occurs.

Fig. 14 shows the stress and strain relation of the critical tensile member. The vertical axis is a non-dimensional parameter σ/σ_y . As the maximum tensile strain, whose point is marked in the figure, does not reach the ultimate strain of 10%, collapse is not caused by tensile failure.

5. Analytical results of progressive collapse analysis of Bridge Model B

Fig. 15 shows the results of progressive collapse analysis and the final deformation of Model Bridge B in the four load cases.

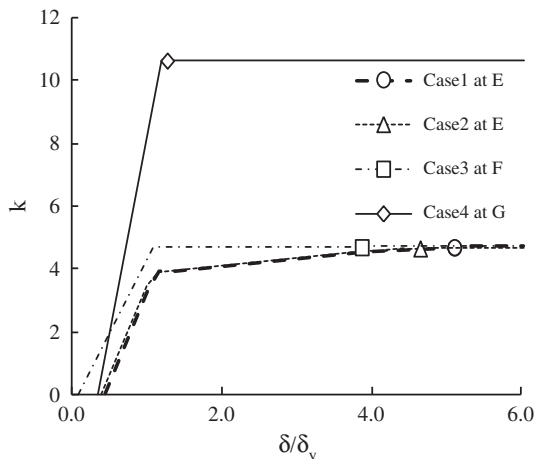


Fig. 13. Live load amplification coefficient and deflection of Bridge Model A.

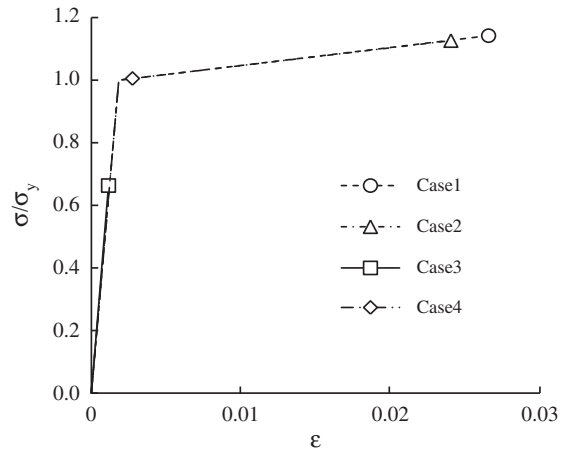


Fig. 14. Tensile stress and strain of Bridge Model A.

In Case-1, the upper chord at support B became yield in tension at first. Then, lower chord became yield in tension at the span center. Next, compression yield appeared near the intermediate support and in the span center. Finally, when the load amplification coefficient k reached 4.70, the upper chord buckled at the span center. The maximum tensile strain was 1.5% at the upper chord at support B. At collapse the deflection at the center span is very large but the deflection at the side span is small.

In Case-2, the lower chords at the span center became yield in tension at first. Then, the upper chord at support B became yield in tension. Finally, when the load amplification coefficient k reached 4.65, the upper chord buckled at the span center. The maximum tensile strain was 1.4% at the lower chord in the span center. At collapse the deflection at the center span is very large but the deflection at the side span is small.

In Case-3, the lower chord at the side span became yield in tension at first. Then, the upper chord at support B became yield in tension. Finally, when the load amplification coefficient k reached 5.79, the upper chord buckled at the side span. The maximum tensile strain was 3.4% at the upper chord at the side span. At collapse the deflection at the side span is very large but the deflection at the center span is small.

In Case-4, the upper chord at support B became yield in tension when load amplification coefficient k reached 7.90. Then, the diagonal member near support B became yield in tension. Finally, when the load amplification coefficient k reached 8.26, the diagonal member buckled at support B. The maximum tensile strain was 0.2% at the diagonal member near support B. When the increment k increased by 0.01, the center span sharply fell underneath because of the buckling at support B which is the same as in Bridge Model A.

Fig. 16 shows the compressive stress and strain relation of the buckled members. The vertical axis is a non-dimensional parameter σ/σ_y . The bridge collapsed at σ/σ_y of -1.11 in Case-1, -1.11 in Case-2, -1.03 in Case-3 and -1.10 in Case-4. These results show that the model truss bridge collapsed because of buckling after it reached the yield stress.

Fig. 17 shows relationship of applied loads and vertical displacements at the critical points. The load amplification coefficient k instead of the load itself is used so as to compare the four live load cases. Lateral axis is a non-dimensional parameter δ/δ_y . In all the cases vertical displacements sharply increase when they reach the yield loads and then increase further after buckling occurs. The value of δ/δ_y at the buckling, whose points are marked in the figure, is 4.88, 4.55, 11.81 and 1.75 in Cases-1, 2, 3, 4, respectively.

Fig. 18 shows the stress and strain relation of the critical tensile members. The vertical axis is a non-dimensional parameter σ/σ_y . As the maximum tensile strain does not reach the ultimate strain of 10%, collapse is not caused by tensile failure.

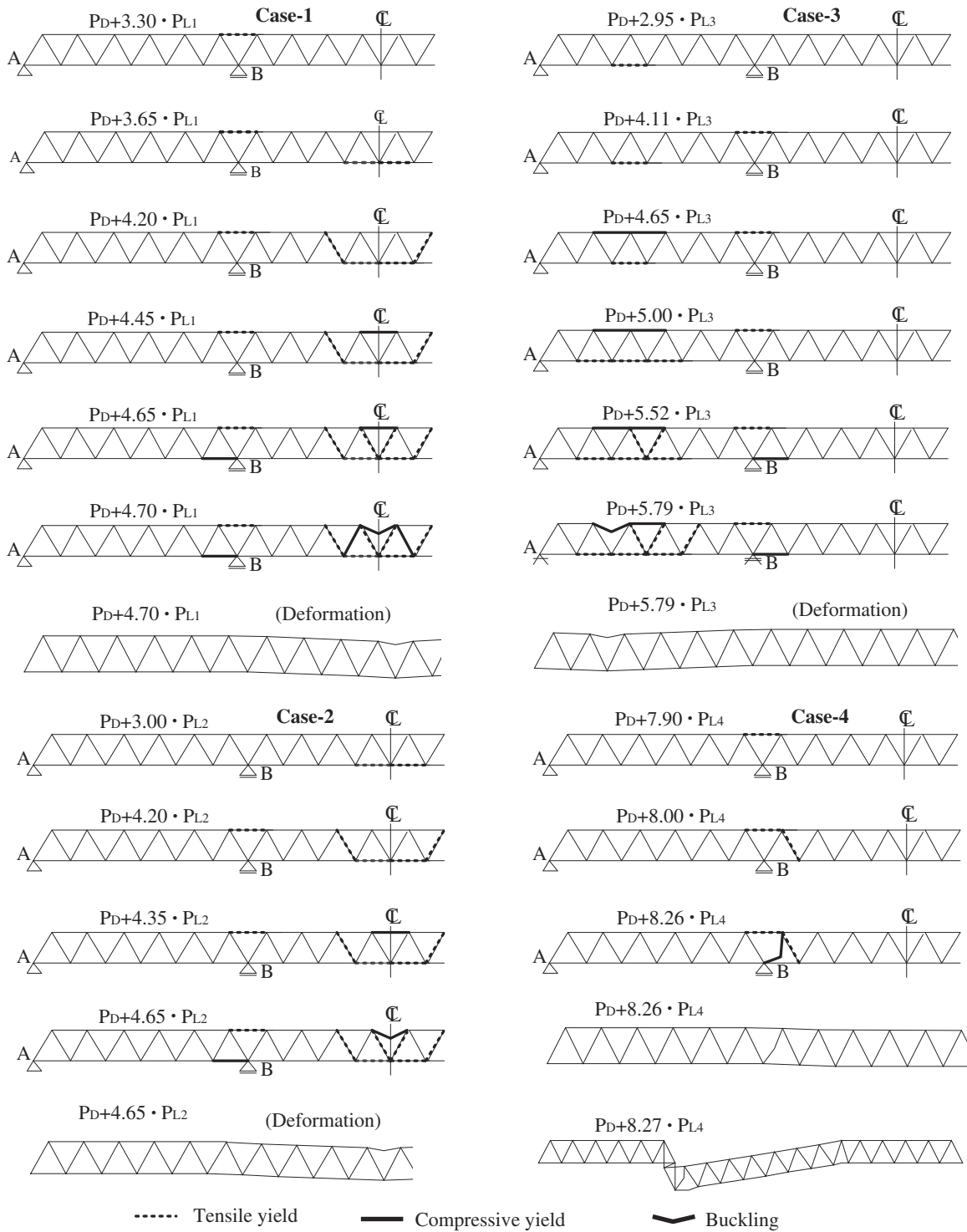


Fig. 15. Collapse process and final deformation of Bridge Model B.

6. Ductility evaluation

In the previous sections, progressive collapse analysis was conducted for the two bridge models with different span ratios. It shows that collapse process and deformation depend on the span ratio and the live load distribution.

In this section, ductility of the two bridge models is evaluated in the four load cases. Ductility of the bridge models is evaluated as shown below. The live load amplification coefficient is expressed as k_y when a first yield member appears. Then, the live load increment

coefficient is expressed as k_u when buckling occurs. Ductility factor of the bridge model μ is defined by a fraction of k_u over k_y .

Tables 4 and 5 show k_y , k_u and ductility factor μ . In Case 1, the ductility factor μ of Bridge Model A and B is both 1.42. In Case-2, that of Bridge Model B is 1.55, which is larger than that of Bridge Model A, 1.35. In Case-3, that of Bridge Model B is 1.96, which is larger than that of Bridge Model A, 1.07. In Case-4, that of Bridge Model B is 1.05, which is smaller than that of Bridge Model A, 1.07. Except in Case-4 which is an extraordinary load case, Bridge Model B is in general more ductile than Bridge Model A.

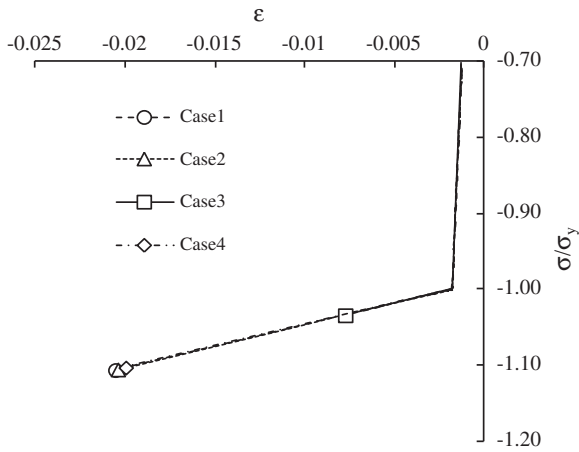


Fig. 16. Compressive stress and strain of Bridge Model B.

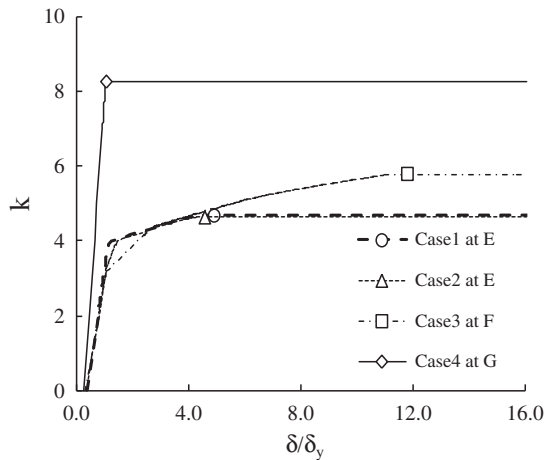


Fig. 17. Live load amplification coefficient and deflection of Bridge Model B.

Table 6 shows the number of yield members when the buckling occurs. After the first member yields, further loads are transferred to other members, in other words, they are redistributed. If there are many yield members at collapse, it means that applied load is redistributed effectively. In Case-1 and Case-2 where live loads are fully applied in the main span, both bridge models collapse due to the buckling of upper chord at mid-span and number of yield

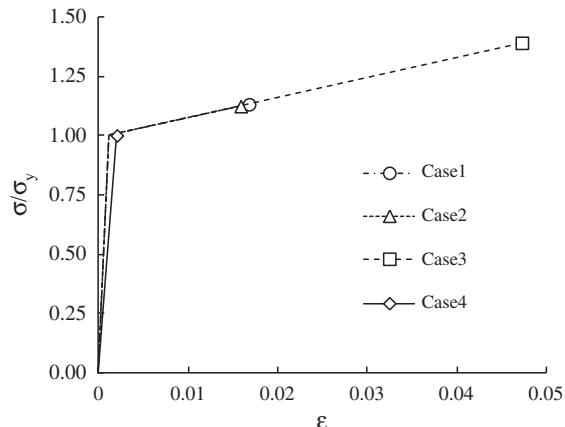


Fig. 18. Tensile stress and strain of Bridge Model B.

Table 4
Ductility of Bridge Model A.

Model A	k_y	k_u	$\mu = k_u/k_y$
Case-1	3.3	4.69	1.42
Case-2	3.45	4.66	1.35
Case-3	4.4	4.7	1.07
Case-4	8.47	11.64	1.37

Table 5
Ductility of Bridge Model B.

Model B	k_y	k_u	$\mu = k_u/k_y$
Case-1	3.3	4.7	1.42
Case-2	3	4.65	1.55
Case-3	2.95	5.79	1.96
Case-4	7.9	8.26	1.05

members was more than 11 at buckling. The number of yield members in Case-3 is 11 for Bridge Model B but 4 for Bridge Model A and, therefore, Bridge Model B is more effective. In Case-4, number of yield members is only 3 for both bridge models, which suggests the failure occurs locally and the load redistribution is small.

7. Discussion and conclusions

In this study, progressive collapse analysis for a three-span continuous Warren truss bridge with total span length of 230 m was carried out for two different center and side span ratios and with four different live load distributions. The collapse process is clarified by the large deformation elastic–plastic method. The collapse process is different depending on live load distribution and length of each span. Especially, it is aimed to clarify the collapse process, the collapse load and the final deformation, furthermore, how the span ratio and the live load distribution affect the truss bridge ductility.

In Case-1 and Case-2 where live loads are fully applied in the center span, Bridge Models A and B collapse due to the buckling of upper chord at the center span. The collapse process and the ultimate strength of Bridge Models A and B are almost the same and the side and center span ratio does not have an effect. The ductility factor μ of the bridge model is defined by the live load amplification coefficient k_u at the buckling over the live load amplification coefficient k_y when a first yield member appears. The ductility factor is over 1.35 and both models can be thought sufficiently ductile. The number of yield members is more than 11 at buckling and the applied load seems to be redistributed effectively.

In Case-3 where live loads are fully applied only in the side span, Bridge Models A and B collapse due to the buckling of the upper chord at the span center. Although the collapse process of both bridge models are almost the same, the ultimate strength and the ductility factor of Bridge Model B is higher than those of Bridge Model A and, therefore, longer side span improves these properties. The number of yield members of Bridge Model B is also much more than that of Bridge Model A.

In Case-4 where live loads are applied near the intermediate support, Bridge Models A and B collapse due to the buckling of the diagonal member near the intermediate support. Although the collapse process of both bridge models are almost the same, the ultimate

Table 6
Number of yield members at collapse.

Load cases	Case-1	Case-2	Case-3	Case-4
Bridge Model A	11	13	4	3
Bridge Model B	13	11	11	3

strength and the ductility factor of Bridge Model A is higher than those of Bridge Model B and, therefore, longer center span improves these properties. The number of yield members of Bridge Model A and B are three, which indicates the failure occurs locally and the load redistribution is small.

The ultimate strain of a tensile member is less than 10% in all the cases. It is therefore concluded that the bridge models do not collapse due to breakage of the tensile members but buckling of the compressive members.

Summarizing the above results, bridge models collapse due to buckling of the compressive member in all the cases. When the live load is fully applied in the center span, the span ratio does not affect the ultimate strength which is sufficiently high. When the live load is applied in the side span, the model bridge with a longer side span has higher ultimate strength. When the live load is applied near the intermediate support, the model bridge with a longer center span has higher ultimate strength. As for ductility factor, Bridge Model B is in general more ductile than Bridge Model A. This leads to the conclusion that the center and side span length ratio of more commonly used truss bridges is rational.

Other researchers have studied the collapse of truss bridge, focusing global redundancy or local buckling of gusset plates. The present study is new because it clarifies the collapse process, buckling strength, and effects of live load distribution and the span ratio.

References

- [1] National Transportation Safety Board. Highway Accident Report, Collapse of I-35W Highway Bridge, Minneapolis, Minnesota August 1, 2007; 2008-11-14. NTSB/HAR-08/03PB 2008-916203.
- [2] Wildey Jim. Bridge Description and Collapse. (cited 2010. 3.6) NTSB report. http://www.nts.gov/events/2008/Minneapolis-MN/2_edited_Board_presentation_Wildey_graphic.ppt.
- [3] T.Tamakoshi: Results of the technical investigation group for the bridge collapse in USA, Constructional Management Technology, pp.39–44, 2008.1.
- [4] H.Nagatani, N.Akashi, T.Matsuda, M.Yasuda, H.Ishii, M.Miyamori, Y.Obata, H.Hirayama, Y.Okui: Redundancy analysis of Japanese steel truss bridges, Proc Jpn Civ Eng Assoc A, Vol.65 No.2, 410–425, 2009.5.
- [5] Kasano H, Yoda T. Collapse mechanism and evaluation of node damages of I-35W Bridge, Minneapolis, USA. Proc Jpn Civ Eng Assoc A 2010;66(2):312–23.
- [6] Japan Road Association: Specifications for Road Bridges, I. General, II. Steel Bridges, (2002.3).